PMA or PMA in the presence of CYLD knockdown for 2–3 hours. This allows NF-κB to become active and stimulate expression of the anti-apoptotic NF-κB target genes. Then we add TNF-α and CHX at the same time. The CHX is added because TNF-α has two effects; it induces apoptosis in a transcription-independent fashion, and induces NF-κB to protect from apoptosis, which requires transcription. By adding CHX and TNF-α at the same time, the anti-apoptotic effects of TNF-α are blocked (by CHX), leaving only the apoptotic signalling pathway intact. This is why combined treatment with TNF-α and CHX is such a powerful inducer of apoptosis. Thus, in this experimental set-up the apoptotic effects of TNF-α can only be rescued by activation of NF-κB target genes prior to CHX treatment (that is, through the combined effects of PMA + CYLD knockdown).

Seventy-two hours after electroporation of HeLa cells with the indicated plasmids, cells were treated with 200 nM PMA for 2-3 hours to stimulate NF-κB activity, followed by a 12-hour incubation in medium containing both 10 ng ml^{-1} TNF-α and 10 μg ml^{-1} CHX to induce apoptosis. Viable cells were quantified using the Trypan blue exclusion method. To inhibit NF-κB activity, medium was supplemented with 10 mM sodium salicylate 3.5 hours before TNF-α addition.

1. Wilkinson, K. D. Ubiquitination and deubiquitination: Targeting of proteins for degradation by the proteasome. *Semin. Cell Dev. Biol.* **11**, 141–148 (2000).
2. Chung, C. H. & Baek, S. H. Deubiquitinating enzymes: Their diversity and emerging roles. *Biochem. Biophys. Res. Commun.* **266**, 633–640 (1999).
3. D'Andrea, A. & Pellman, D. Deubiquitinating enzymes: A new class of biological regulators. *Crit. Rev. Biochem. Mol. Biol.* **33**, 337–352 (1998).
4. Bignell, G. R. et al. Identification of the familial cylindromatosis tumour-suppressor gene. *Nature Genet.* **25**, 160–165 (2000).
5. Yin, M. J., Yamamoto, Y. & Gaynor, R. B. The anti-inflammatory agents aspirin and salicylate inhibit the activity of IκB kinase-β. *Nature* **396**, 77–80 (1998).
6. Nakamura, T., Hillova, J., Mariage-Samson, R. & Hill, M. Molecular cloning of a novel oncogene generated by DNA recombination during transfection. *Oncogene Res.* **2**, 357–370 (1988).
7. Papa, F. R. & Hochstrasser, M. The yeast *DOA4* gene encodes a deubiquitinating enzyme related to a product of the human *tre-2* oncogene. *Nature* **366**, 313–319 (1993).
8. Brummelkamp, T. R., Bernards, R. & Agami, R. A system for stable expression of short interfering RNAs in mammalian cells. *Science* **296**, 550–553 (2002).
9. Karin, M., Cao, Y., Greten, F. R. & Li, Z. W. NF-κB in cancer: From innocent bystander to major culprit. *Nature Rev. Cancer* **2**, 301–310 (2002).
10. Smahi, A. et al. The NF-κB signalling pathway in human diseases: From incontinentia pigmenti to ectodermal dysplasias and immune-deficiency syndromes. *Hum. Mol. Genet.* **11**, 2371–2375 (2002).
11. Trompouki, E. et al. CYLD is a deubiquitinating enzyme that negatively regulates NF-kB activation by TNFR family members. *Nature* **424**, 793–796 (2003).
12. Bradley, J. R. & Pober, J. S. Tumor necrosis factor receptor-associated factors (TRAFs). *Oncogene* **20**, 6482–6491 (2001).
13. Chung, J. Y., Park, Y. C., Ye, H. & Wu, H. All TRAFs are not created equal: Common and distinct molecular mechanisms of TRAF-mediated signal transduction. *J. Cell Sci.* **115**, 679–688 (2002).
14. Shi, C. S. & Kehrl, J. H. TNF-induced GCKR and SAPK activation depends upon the E2/E3 complex Ubc13-Uev1A/TRAF2. *J. Biol. Chem.* **18**, 15429–15434 (2003).
15. Wang, C. et al. TAK1 is a ubiquitin-dependent kinase of MKK and IKK. *Nature* **412**, 346–351 (2001).
16. Holtmann, H., Hahn, T. & Wallach, D. Interrelated effects of tumor necrosis factor and interleukin 1 on cell viability. *Immunobiology* **177**, 7–22 (1988).
17. Wang, C. Y., Mayo, M. W. & Baldwin, A. S. Jr TNF- and cancer therapy-induced apoptosis: Potentiation by inhibition of NF-κB. *Science* **274**, 784–787 (1996).
18. Liu, Z. G., Hsu, H., Goeddel, D. V. & Karin, M. Dissection of TNF receptor 1 effector functions: JNK activation is not linked to apoptosis while NF-κB activation prevents cell death. *Cell* **87**, 565–576 (1996).
19. De Smaele, E. et al. Induction of gadd45β by NF-κB downregulates pro-apoptotic JNK signalling. *Nature* **414**, 308–313 (2001).
20. Baud, V. & Karin, M. Signal transduction by tumor necrosis factor and its relatives. *Trends Cell Biol.* **11**, 372–377 (2001).
21. Rossi, A. et al. Anti-inflammatory cyclopentenone prostaglandins are direct inhibitors of IκB kinase. *Nature* **403**, 103–108 (2000).
22. Dajee, M. et al. NF-κB blockade and oncogenic Ras trigger invasive human epidermal neoplasia. *Nature* **421**, 639–643 (2003).
23. van Balkom, I. D. & Hennekam, R. C. Dermal eccrine cylindromatosis. *J. Med. Genet.* **31**, 321–324 (1994).
24. Schmidt-Ullrich, R. et al. NF-κB activity in transgenic mice: Developmental regulation and tissue specificity. *Development* **122**, 2117–2128 (1996).
25. Schmidt-Ullrich, R. et al. Requirement of NF-κB/Rel for the development of hair follicles and other epidermal appendices. *Development* **128**, 3843–3853 (2001).
26. Agami, R. & Bernards, R. Distinct initiation and maintenance mechanisms cooperate to induce G1 cell cycle arrest in response to DNA damage. *Cell* **102**, 55–66 (2000).
27. Chen, G., Cao, P. & Goeddel, D. V. TNF-induced recruitment and activation of the IKK complex require Cdc37 and Hsp90. *Mol. Cell* **9**, 401–410 (2002).

The tumour suppressor CYLD negatively regulates NF-κB signalling by deubiquitination

Andrew Kovalenko[1,2], Christine Chable-Bessia[2], Giuseppina Cantarella[1,3], Alain Israël[2], David Wallach[1] & Gilles Courtois[2]

[1]*Department of Biological Chemistry, The Weizmann Institute of Science, 76100 Rehovot, Israel*
[2]*Unité de Biologie Moléculaire de l'Expression Génique, CNRS URA 2582, Institut Pasteur, 75015 Paris, France*
[3]*Department of Experimental and Clinical Pharmacology, University of Catania School of Medicine, I-95125 Catania, Italy*

NF-κB transcription factors have key roles in inflammation, immune response, oncogenesis and protection against apoptosis[1,2]. In most cells, these factors are kept inactive in the cytoplasm through association with IκB inhibitors. After stimulation by various reagents, IκB is phosphorylated by the IκB kinase (IKK) complex[3] and degraded by the proteasome, allowing NF-κB to translocate to the nucleus and activate its target genes. Here we report that CYLD, a tumour suppressor that is mutated in familial cylindromatosis[4], interacts with NEMO, the regulatory subunit of IKK[5,6]. CYLD also interacts directly with tumour-necrosis factor receptor (TNFR)-associated factor 2 (TRAF2), an adaptor molecule involved in signalling by members of the family of TNF/nerve growth factor receptors. CYLD has deubiquitinating activity that is directed towards non-K48-linked polyubiquitin chains, and negatively modulates TRAF-mediated activation of IKK, strengthening the notion that ubiquitination is involved in IKK activation by TRAFs and suggesting that CYLD functions in this process. Truncations of CYLD found in cylindromatosis result in reduced enzymatic activity, indicating a link between impaired deubiquitination of CYLD substrates and human pathophysiology.

The regulatory subunit of IKK, NEMO (also known as IKK-γ), has an essential role in NF-κB activation and its dysfunction is associated with several distinct human pathologies[7]. On applying the carboxy-terminal half of NEMO as a bait in two-hybrid screening, we found that it bound specifically to the tumour suppressor CYLD (Fig. 1a). CYLD was originally identified through positional cloning of the gene responsible for familial cylindromatosis, an autosomal dominant disease characterized by benign tumours derived from cells of skin appendages, which appear predominantly in hairy areas of the body during adulthood[4].

The binding site for CYLD on NEMO was found to correspond to the last 39 amino acids of the NEMO protein, where a zinc-finger is located (Fig. 1a). In further two-hybrid tests, CYLD was found to bind to TRAF2 but not to other members of the TRAF family or to any of the following signalling proteins: TRADD, RIP, RIP2, NIK, FADD, cFLIP, caspase 8, APAF1, IAP-1, the p55 TNFR intracellular domain, FAS-IC or A20 (data not shown). The whole TRAF domain of TRAF2 seemed to be required for the CYLD–TRAF2 interaction (Fig. 1b). We found that the NEMO-binding site is located between amino acids 470 and 684 in CYLD, whereas the TRAF2-binding site is located between CYLD amino acids 394 and 470. Because TRAF2 binds to the sequence motif Pro-X-Gln-X-(Ser/Thr)[8] and we found a similar sequence in the TRAF2-binding domain of CYLD (Pro 453-Val 454-Gln 455-Glu 456-Ser 457), we examined the participation of this sequence in the TRAF2–CYLD interaction by mutating Ser 457 to alanine. This mutation abolished TRAF2 binding to CYLD (Fig. 1c).

CYLD binding to NEMO and to TRAF2 could be also detected in transfected human embryonic kidney (HEK) 293T cells (Fig. 2a, d).

Notably, the interaction of CYLD with NEMO was associated with the appearance of a shifted band of CYLD (Fig. 2a), representing a phosphorylated form of this molecule (Fig. 2b). The kinase involved did not seem to be IKK (Supplementary Fig. 1). No interaction was detected between CYLD and dC385 NEMO, a truncated version of NEMO lacking the C-terminal zinc-finger, confirming the participation of this domain in CYLD binding (Fig. 2c).

As previously noted[4], CYLD contains two sequence motifs that share similarity with the cysteine and histidine boxes found in the UBP ubiquitin-specific protease subfamily of enzymes with deubiquitinase activity[9,10]. Notably, an evolutionarily conserved motif located at the C terminus of known CYLD orthologues from various species corresponds to subdomain III of the UBP histidine box and is deleted in the shortest truncation of CYLD that generates cylindromatosis[4] (Fig. 3a).

We assessed the effect of transfected CYLD on the overall pattern of cellular protein ubiquitination but observed no obvious reduction in the extent of conjugation of wild-type ubiquitin tagged with an influenza A virus haemagglutinin epitope (HA–ubiquitin) to the cellular proteins. Nor did we observe any effect of CYLD on the conjugation of ubiquitin in which Lys 63 had been replaced with arginine (K63R). By contrast, conjugation of ubiquitin in which Lys 48 had been replaced with arginine (K48R) was markedly reduced (Fig. 3b). These findings suggest that CYLD affects proteins with ubiquitin conjugated through Lys 63 (K63-Ub) but not those with ubiquitin conjugated through Lys 48 (K48-Ub). It cannot be excluded that CYLD also affects other modes of ubiquitin conjugation; for example, through Lys 29.

Both TRAF2 and TRAF6 have been shown to act as E3 ubiquitin ligases and to ubiquitinate themselves through K63-Ub conjugation[11–13]. This modification, in contrast to K48-Ub conjugation, is not associated with proteolysis, but instead triggers signalling through an undefined mechanism[12]. When we co-transfected TRAF2 or TRAF6 with HA–ubiquitin into HEK 293T cells, polyubiquitination of both proteins was indeed observed (Fig. 3c).

Unexpectedly, when NEMO was included in the experiment as another CYLD-interacting protein, it was also polyubiquitinated. As with TRAF2 and TRAF6, inhibition of proteasome function had no effect on the cellular amounts of ubiquitinated NEMO (Supplementary Fig. 2), indicating that this modification does not target it for degradation.

Transfection of CYLD together with NEMO, TRAF2 or TRAF6 resulted in disappearance of the ubiquitinated forms of the three proteins (Fig. 3c). Notably, co-transfection of TRAF2 with a Ser 457-to-alanine mutant of CYLD, (S/A)CYLD, that could not bind TRAF2 resulted in a lower degree of deubiquitination as compared with cells co-transfected with TRAF2 and wild-type CYLD, indicating that the specific binding of TRAF2 to CYLD assists its deubiquitination (Fig. 3d). By contrast, (S/A)CYLD was just as potent as the wild-type protein in its ability to act on either TRAF6 or NEMO (Fig. 3d). The truncated version of CYLD originally isolated during our two-hybrid screen (clone 10 or (ΔN393)CYLD; Fig. 1c) showed a restricted substrate specificity. It could deubiquitinate TRAF2 and NEMO, but not TRAF6 (Supplementary Fig. 3). CYLD also showed deubiquitinating activity in a cell-free assay (Fig. 3e). Replacement of the putative catalytic histidine residue of CYLD (Fig. 3a) by an asparagine residue, (H/N)CYLD, resulted in total loss of its activity, showing that the enzymatic activity of CYLD, rather than interference caused by binding to NEMO or TRAF2, was responsible for the observed effect (Fig. 3c, e). CYLD did not affect the K48-linked ubiquitination of β-catenin or IκBα (refs 1, 14, and Fig. 3f), further indicating that it functions as a K63-Ub-specific deubiquitinase.
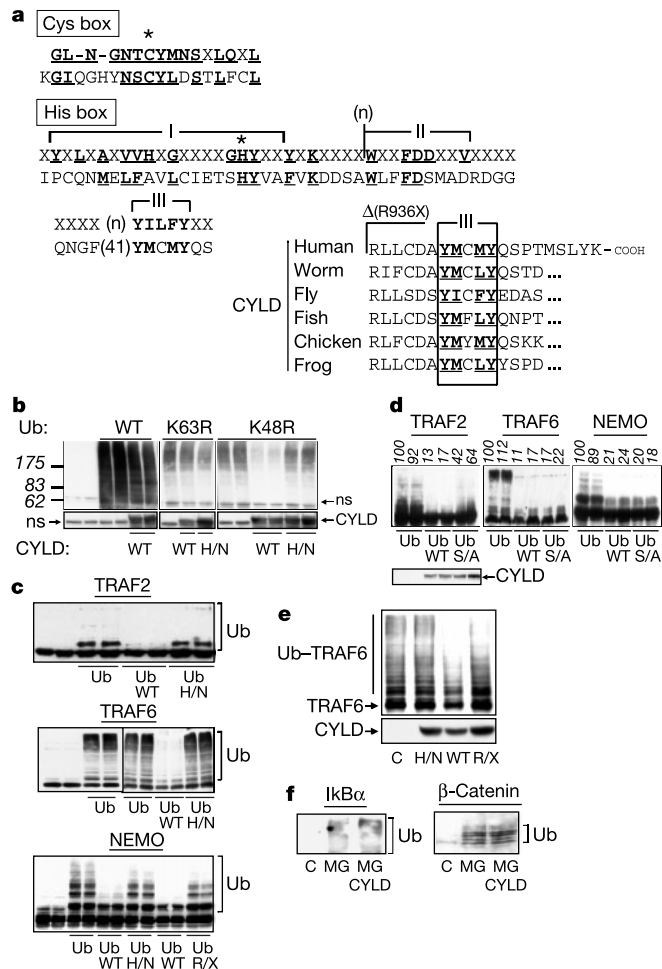
As discussed above, the shortest truncation of CYLD that generates cylindromatosis (introduction of a stop codon at Arg 936) eliminates subdomain III of the histidine box[4]. We therefore examined the impact of this mutation, (R/X)CYLD, on the enzymatic activity of CYLD. We observed a severe reduction in deubiquitinase activity of (R/X)CYLD both in transfected cells and in a cell-free assay (Fig. 3c, e). This confirms the role of this domain
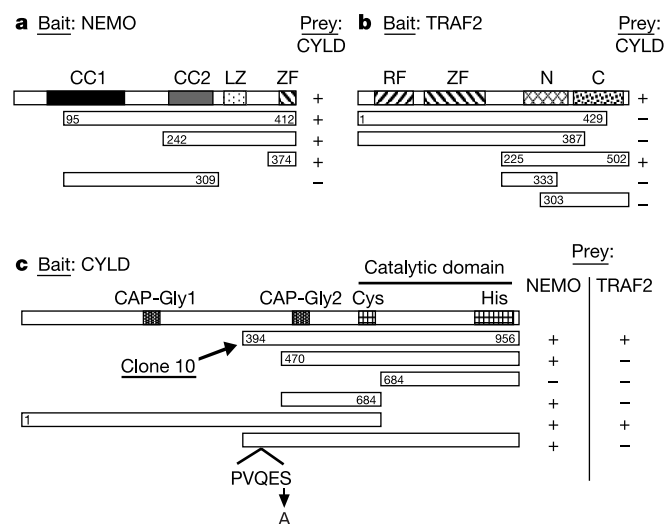
Figure 1 Mapping the binding of CYLD to NEMO and TRAF2 in yeast. Interactions between the fusion proteins were assessed by filter assays for β-galactosidase activity. The plus sign indicates activity within 2 h and the minus sign indicates no activity within 24 h. Amino-acid coordinates of the deletion mutants of NEMO (**a**), TRAF2 (**b**) and CYLD (**c**) are indicated. CC, coiled-coil; LZ, leucine zipper; ZF, zinc-finger; RF, RING-finger; N, TRAFN domain; C, TRAFC domain; CAP-Gly, putative microtubule-binding motif[4]; Cys and His, cysteine and histidine boxes of the UBP catalytic domain; clone 10, the original cDNA clone identified in the two-hybrid screening.
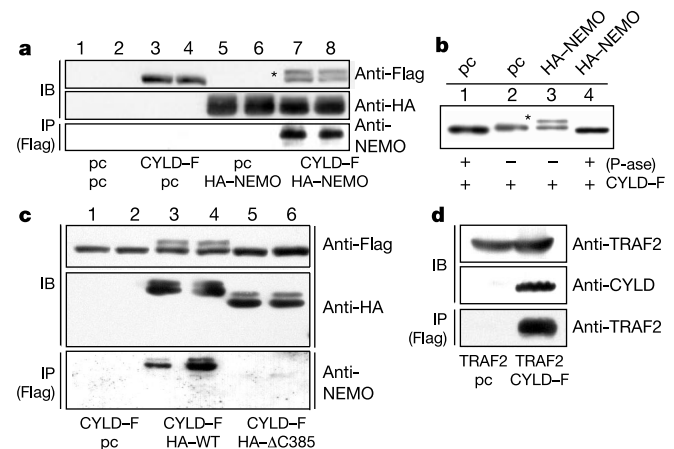
Figure 2 *In vivo* interaction of CYLD with NEMO and TRAF2. **a**, Interaction between CYLD and NEMO. HEK 293T cells were transfected with the indicated combinations of empty vector (pc) and expression constructs encoding HA–NEMO or CYLD–Flag (CYLD-F). Cell extracts were analysed by immunoblotting either directly (IB) or after immunoprecipitation with antibodies against Flag (IP). Asterisk indicates a retarded CYLD species. **b**, NEMO–CYLD interaction results in phosphorylation of CYLD. Lysates of HEK 293T cells transfected with the indicated constructs were incubated without or with λ-phosphatase (P-ase), and then analysed directly by immunoblotting with antibodies against Flag. **c**, The zinc-finger of NEMO is required for interaction with CYLD. The experiment was done as in **a**; HA–WT, full-length NEMO; HA–ΔC385, NEMO lacking the zinc-finger. **d**, Interaction between CYLD and TRAF2. Extracts were analysed by immunoblotting either directly (IB) or after immunoprecipitation with antibodies against Flag (IP).

in the deubiquitinase activity and suggests that cylindromatosis pathology results from defective deubiquitination of *in vivo* CYLD substrates.

We assessed the affect of overexpressing CYLD on TNF and interleukin-1 (IL-1) function and found that it inhibited the induction of NF-κB by both cytokines (Fig. 4a). This inhibition was diminished when the enzymatically inactive mutant (H/N)CYLD was used instead of wild-type CYLD (Fig. 4a). Overexpression of the mutant (S/A)CYLD, which does not bind TRAF2, also decreased the inhibitory effect of CYLD on NF-κB activation induced by TNF, which involves TRAF2, but not its inhibitory effect on NF-κB activation induced by IL-1, which involves TRAF6 (Fig. 4a).

Overexpression of CYLD also substantially inhibited NF-κB activation induced by several members of the TNFR and IL-1 receptor/Toll-like receptor families, including TNFR-1, EDAR and TLR4 (Fig. 4b), as well as by LMP1, TRAF2, TRAF5, TRAF6, RIP, TRADD and Myd88, of which the effect on TRAF2 was the strongest (Fig. 4c). (H/N)CYLD was only slightly inhibitory to these signalling proteins, whereas (ΔN393)CYLD strongly inhibited TRAF2- but not TRAF6-dependent activation of NF-κB (Supplementary Fig. 3).

Notably, when NF-κB was activated by NIK (a kinase that binds to and activates IKK1; ref. 15), by Tax (a viral protein that directly interacts with NEMO and activates IKK[16]), or by a constitutively active form of IKK2 (IKK2(E/E)[17]), the overexpressed CYLD was barely inhibitory and no difference was seen between wild-type and
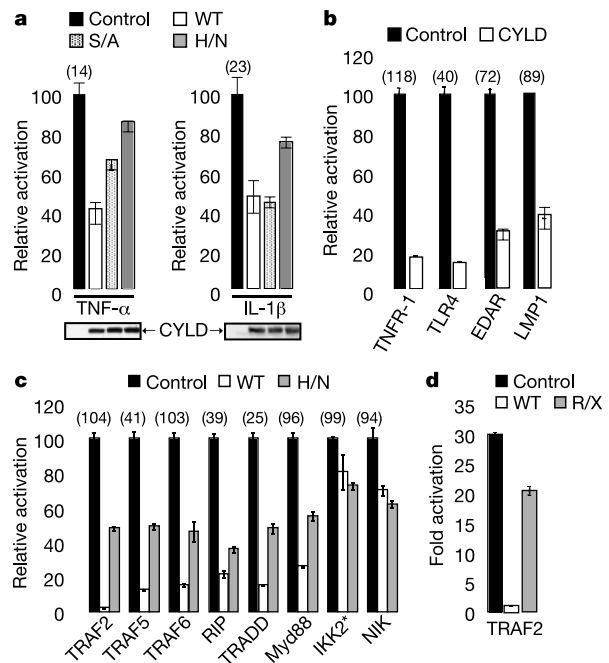
Figure 3 CYLD is an active UBP deubiquitinase with restricted substrate specificity. **a**, Top, alignment of CYLD fragments (lower row) with the consensus of the UBP family, and conserved residues in UBP proteins (see the Protein families database of alignments and HMMs (Pfam) at http://www.sanger.ac.uk/Software/Pfam). Asterisks indicate cysteine and histidine residues implicated in the catalytic mechanism, n indicates a variation in amino-acid number between UBP proteins. Bottom, degree of evolutionary conservation in the C-terminal region of CYLD corresponding to block III of the histidine box, and the site of the most distal mutation (R936X) found in cylindromatosis (family TT17), which results in truncation of the last 20 residues of CYLD[4]. **b**, CYLD is a deubiquitinating enzyme affecting non-K48–linked ubiquitination. HA-tagged human wild-type, K48R or K63R ubiquitin was co-transfected with empty vector or a construct expressing wild-type CYLD (WT) or catalytically inactive CYLD (H/N). Overall protein ubiquitination (top) and the expression of CYLD (bottom) were assessed by immunoblotting with antibodies against HA and Flag, respectively. ns, nonspecific signal. Results are representative of three independent experiments exposed to achieve similar signal intensities. **c**, CYLD can deubiquitinate TRAF6, TRAF2 and NEMO *in vivo*. HEK 293T cells were transfected with pCMV–Flag–TRAF6, pCMV–HA–NEMO or pCMV–HA–TRAF2, plus empty vector or a pCMV–HA–ubiquitin (Ub) plasmid. The effect of wild-type CYLD, His-box-mutated CYLD (H/N), or C-terminally truncated CYLD (R/X) on ubiquitinated molecules was assessed by immunoblotting with antibodies against TRAF6, NEMO or TRAF2. **d**, TRAF2 deubiquitination by CYLD is controlled by their specific interaction. Conditions were similar to those in **c**. S/A is the Flag-tagged S457A CYLD mutant. Numbers indicate the relative extent of ubiquitination. The relative expression of transfected CYLD constructs is shown below. **e**, CYLD has deubiquitination activity in a cell-free assay. Equal amounts of wild-type CYLD or the two CYLD mutants (H/N, R/X) obtained from transfected cell lysates were incubated with Flag–TRAF6 beads in deubiquitination buffer (Methods). TRAF6 ubiquitination was analysed with antibodies against TRAF6. **f**, CYLD does not affect the ubiquitination of IκBα or β-catenin. The analysis was done essentially as in **c**, except that cells were pretreated with the proteasomal inhibitor MG132 (MG) to allow ubiquitinated molecules to accumulate for detection. IκBα ubiquitination was induced by co-transfecting cells with IKK2(E/E)[17] and detected with antibodies against IκBα. Ubiquitination of β-catenin was detected with antibodies against β-catenin after immunoprecipitation with antibodies against HA.
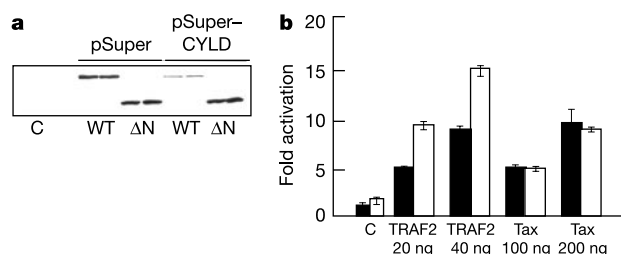
Figure 4 Overexpression of CYLD inhibits NF-κB activation and this inhibition requires its catalytic activity. **a**, CYLD-mediated inhibition of NF-κB activation by TNF-α or IL-1β. HEK 293T cells were co-transfected with either empty vector (control) or constructs expressing wild-type CYLD, (S/A)CYLD and (H/N)CYLD, and NF-κB activation was analysed by a luciferase assay after stimulation with TNF-α or IL-1β (10 ng ml^{−1} for 4 h). Results are representative of at least two experiments done in duplicate; bars indicate the s.d. in each series. Relative expression of the CYLD constructs is shown below the luciferase data. **b**, CYLD-mediated inhibition of NF-κB activation by members of the TNFR and IL-1 receptor families. Analysis was done as in **a**, except that NF-κB was activated by overexpressing the indicated receptors. Relative stimulation is shown; numbers indicate the absolute fold activation. **c**, CYLD-mediated inhibition of NF-κB activation by signalling intermediates. Analysis was done as in **a**. **d**, (R/X)CYLD does not inhibit NF-κB activation. Analysis was done as in **a**, using TRAF2 as activator of NF-κB.

(H/N)CYLD (Fig. 4c and data not shown). This indicates that the overexpressed CYLD is not acting by directly inhibiting the IκBα ubiquitination step (see also Fig. 3f), the subsequent IκB degradation step, or probably the final step of IKK activation, but rather functions by inhibiting an upstream event that is required for this activation. Indeed, although it effectively blocked degradation of IκB induced by TNF treatment, CYLD had no effect on the phosphorylation of IκB nor on its degradation in response to IKK2(E/E) expression (Supplementary Fig. 4). (R/X)CYLD did not seem to inhibit NF-κB activation (Fig. 4d), further showing that the negative regulation of NF-κB activation by CYLD is dependent on its catalytic activity.

To confirm the negative role of CYLD in TRAF-dependent NF-κB activation, we tried to reduce endogenous CYLD expression through RNA-mediated (RNAi) interference[18] using a pSUPER expression vector (pSUPER–CYLD)[19]. Expression of exogenous full-length CYLD, but not of a CYLD truncation mutant lacking the short interfering RNA (siRNA) target site (ΔN), was markedly decreased by expression of this vector (Fig. 5a), showing its efficiency and specificity in reducing CYLD expression. When transfected with pSUPER–CYLD, HEK 293T cells showed a roughly twofold increase in the activation of NF-κB induced by small amounts of TRAF2. By contrast, the same amount of NF-κB activation induced by Tax was not changed by expression of the CYLD siRNA, indicating that the effect was specific (Fig. 5b).

Our study shows that the tumour suppressor CYLD is a member of the UBP class of deubiquitinating enzymes that preferentially cleaves non-K48-Ub-conjugated moieties and negatively regulates NF-κB activation. While this manuscript was in preparation, CYLD was shown to possess deubiquitinating activity on the basis of experiments using active-site-directed inhibitors of deubiquitinating enzymes[20]. Our data indicate that TRAF2 and NEMO are *in vivo* targets of CYLD. The association of CYLD with NEMO and TRAF2, and probably also cytoskeletal associations imposed on CYLD by its CAP-Gly motifs[4], may allow it to specifically affect other target proteins. Despite our still limited knowledge of the identity of the CYLD substrates, our findings clearly indicate that this molecule controls the ubiquitination of signalling proteins that function upstream of IKKs, thereby identifying an additional stage of regulation in the NF-κB pathway. CYLD dysfunction at this stage may result in excessive activation of NF-κB and trigger cell transformation through increased resistance to apoptosis or perturbation of the cell cycle[21]. □

Methods

Yeast two-hybrid screening

A complementary DNA corresponding to the C-terminal part of the human NEMO open reading frame (ORF; nucleotides 284–1260) was cloned into the GAL4 DNA-binding domain (DBD) vector pGBT9 (Clontech). The resulting plasmid pGBT9–NEMO was used as bait in a two-hybrid screen of a human B-cell cDNA library (Clontech) in *Saccharomyces cerevisiae* HF7c. Isolation of positive clones and subsequent two-hybrid interaction analyses using a Matchmaker TwoHybrid System Protocol (Clontech) were done according to the manufacturer's instructions. We assessed the binding properties of CYLD and other proteins in the yeast SFY526 reporter strain (Clontech) using the pGBT9-GAL4-DBD and pGAD-GH-GAL4-AD vectors. Deletion constructs for two-hybrid mapping were made by conventional polymerase chain reaction (PCR).

Antibodies and expression constructs

We used antibodies against TRAF2 (H-249, Santa Cruz), TRAF6 (H-274, Santa Cruz), NEMO (PharMingen and ref. 5), the Flag epitope (M2, Sigma), the HA epitope (a homemade hybridoma), β-catenin (Sigma) and IκBα (Transduction Laboratories).

The wild-type ubiquitin expression vector encoding an octameric tandem fusion of HA–ubiquitin was a gift from M. Treier (EMBL). Both the K48R and K63R HA–ubiquitin point mutants in a bacterial expression vector were a gift from K.-I. Nakayama (Kyushu University). For the mammalian expression experiments, we transferred a single copy of each of the mutant cDNAs into the pcDNA3 vector by using conventional cloning techniques.

A cDNA comprising the complete ORF of CYLD was obtained by joining the original two-hybrid clone (clone 10) and a partially overlapping 5′-extending clone obtained from the IMAGE consortium. The resulting full-length cDNA was used to amplify by PCR the predicted CYLD ORF, which was subsequently transferred into a pcDNA3 mammalian expression vector (Invitrogen) that had been modified to include in-frame amino-terminal AU1 and C-terminal Flag epitopes.

We prepared all deletions and point mutants by conventional PCR and cloning techniques. The CYLD R936X deletion construct was derived directly from the C-terminally tagged plasmid pcCYLDwt–Flag and thus contained no epitope tag at its C terminus. For this reason, the activity of this construct was always compared with that of untagged wild-type CYLD.

Cell culture and transfection

HEK 293T cells were transfected as described[22]. We carried out immunoblot analysis, immunoprecipitations and luciferase assays as described[5].

In vitro deubiquitination assay

Both the enzyme (CYLD–Flag) and the substrate (Flag–TRAF6) were expressed separately in HEK 293T cells in 10-cm dishes. After immunoprecipitation with antibodies against Flag, CYLD was eluted by incubation with Flag peptide (Sigma) and added to Flag–TRAF6 beads. The deubiquitination reaction was carried out in 100 μl of deubiquitination buffer (20 mM Tris-HCl (pH 7.5), 5 mM MgCl₂ and 2 mM dithiothreitol) at 30 °C for 1 h. We resolved the reaction products by conventional SDS–PAGE and analysed them by immunoblotting.

CYLD siRNA expression vector

The RNAi procedure was done as described[19]. In brief, a double-stranded oligonucleotide was designed to contain a sequence derived from the 5′ end of human CYLD ORF (nucleotides 232–250) in forward and reverse orientation separated by a 9-base-pair spacer region (ttcaagaga) to allow formation of the hairpin structure in the expressed oligo-RNA: sense strand, 5′-gatccccCCTCATGCAGTTCTCTTTGttcaagagaCAAAGA GAACTGCATGAGGttttttggaaa; antisense strand, 5′-agcttttccaaaaaCCTCATGCAGTT CTCTTTGtctcttgaaCAAAGAGAACTGCATGAGGggg. The resulting double-stranded oligonucleotide was cloned into the *Bgl*II and *Hin*dIII sites of the pSUPER vector for expression under the control of the H1 RNA promoter.

1. Karin, M. & Ben-Neriah, B. Phosphorylation meets ubiquitination: the control of NF-κB activity. *Annu. Rev. Immunol.* **18,** 621–663 (2000).
2. Li, Q. & Verma, I. M. NF-κB regulation in the immune system. *Nature Rev. Immunol.* **2,** 725–734 (2002).
3. Israël, A. The IKK complex: an integrator of all signals that activate NF-κB? *Trends Cell. Biol.* **10,** 129–133 (2000).
4. Bignell, G. R. *et al.* Identification of the familial cylindromatosis tumour-suppressor gene. *Nature Genet.* **25,** 160–165 (2000).
5. Yamaoka, S. *et al.* Complementation cloning of NEMO, a component of the IκB kinase complex essential for NF-κB activation. *Cell* **93,** 1231–1240 (1998).
6. Rothwarf, D. M., Zandi, E., Natoli, G. & Karin, M. IKK-γ is an essential regulatory subunit of the IκB kinase complex. *Nature* **395,** 297–300 (1998).
7. Courtois, G., Smahi, A. & Israël, A. NEMO/IKK-γ: linking NF-κB to human disease. *Trends Mol. Med.* **7,** 427–430 (2001).
8. Ye, H., Park, Y. C., Kreishman, M., Kieff, E. & Wu, H. The structural basis for the recognition of diverse receptor sequences by TRAF2. *Mol. Cell* **4,** 321–330 (1999).
9. Wilkinson, K. D. Regulation of ubiquitin-dependent processes by deubiquitinating enzymes. *FASEB J.* **11,** 1245–1256 (1997).
10. D'Andrea, A. & Pellman, D. Deubiquitinating enzymes: a new class of biological regulators. *Crit. Rev. Biochem. Mol. Biol.* **33,** 337–352 (1998).
11. Deng, L. *et al.* Activation of the IκB kinase complex by TRAF6 requires a dimeric ubiquitin-conjugating enzyme complex and a unique polyubiquitin chain. *Cell* **103,** 351–361 (2000).

Figure 5 CYLD is a negative regulator of the TRAF2 and NF-κB signalling pathway. **a**, CYLD siRNA efficiently blocks expression of transfected CYLD. HEK 293T cells were transiently transfected with either empty pcDNA3 (C) or expression vectors encoding Flag-tagged wild-type CYLD or an N-terminally truncated mutant of CYLD (ΔN; residues 1–393 deleted). CYLD expression was analysed by immunoblotting with a monoclonal antibody against Flag. **b**, Expression of CYLD siRNA potentiates TRAF-dependent activation of NF-κB. HEK 293T cells were co-transfected in duplicate with the indicated amounts of a TRAF2 or Tax expression construct or empty vector (C), plus the Igκ-Luc reporter and either pSUPER–CYLD (open bars) or control pSUPER (filled bars) plasmids. Analysis was done as in Fig. 4.

12. Wang, C. *et al.* TAK1 is a ubiquitin-dependent kinase of MKK and IKK. *Nature* **412**, 346–351 (2001).

13. Shi, C. S. & Kehrl, J. H. TNF-induced GCKR and SAPK activation depends upon the E2/E3 complex Ubc13–Uev1A/TRAF2. *J. Biol. Chem.* **278**, 15429–15434 (2003).

14. Maniatis, T. A ubiquitin ligase complex essential for the NF-κB, Wnt/Wingless, and Hedgehog signaling pathways. *Genes Dev.* **13**, 505–510 (1999).

15. Pomerantz, J. L. & Baltimore, D. Two pathways to NF-κB. *Mol. Cell* **10**, 693–695 (2002).

16. Chu, Z. L., DiDonato, J. A., Hawiger, J. & Ballard, D. W. The tax oncoprotein of human T-cell leukemia virus type 1 associates with and persistently activates IκB kinases containing IKKα and IKKβ. *J. Biol. Chem.* **273**, 15891–15894 (1998).

17. Mercurio, F. *et al.* IKK-1 and IKK-2: cytokine-activated IκB kinases essential for NF-κB activation. *Science* **278**, 860–866 (1997).

18. McManus, M. T. & Sharp, P. A. Gene silencing in mammals by small interfering RNAs. *Nature Rev. Genet.* **3**, 737–747 (2002).

19. Brummelkamp, T. R., Bernards, R. & Agami, R. A system for stable expression of short interfering RNAs in mammalian cells. *Science* **296**, 550–553 (2002).

20. Borodovsky, A. *et al.* Chemistry-based functional proteomics reveals novel members of the deubiquitinating enzyme family. *Chem. Biol.* **9**, 1149–1159 (2002).

21. Karin, M., Cao, Y., Greten, F. R. & Li, Z. W. NF-κB in cancer: from innocent bystander to major culprit. *Nature Rev. Cancer* **2**, 301–310 (2002).

22. Döffinger, R. *et al.* X-linked anhidrotic ectodermal dysplasia with immunodeficiency is caused by impaired NF-κB signaling. *Nature Genet.* **27**, 277–85 (2001).

....

Rationalization of the effects of mutations on peptide and protein aggregation rates

Fabrizio Chiti[1]*, **Massimo Stefani**[2], **Niccolò Taddei**[2], **Giampietro Ramponi**[2] & **Christopher M. Dobson**[1]

[1]*Department of Chemistry, University of Cambridge, Lensfield Road, Cambridge CB2 1EW, UK*
[2]*Dipartimento di Scienze Biochimiche, Università degli Studi di Firenze, Viale Morgagni 50, 50134 Firenze, Italy*

* Present address: Dipartimento di Scienze Biochimiche, Università degli Studi di Firenze, Viale Morgagni 50, 50134 Firenze, Italy

....

In order for any biological system to function effectively, it is essential to avoid the inherent tendency of proteins to aggregate and form potentially harmful deposits[1–4]. In each of the various pathological conditions associated with protein deposition, such as Alzheimer's and Parkinson's diseases, a specific peptide or protein that is normally soluble is deposited as insoluble aggregates generally referred to as amyloid[2,3]. It is clear that the aggregation process is generally initiated from partially or completely unfolded forms of the peptides and proteins associated with each disease. Here we show that the intrinsic effects of specific mutations on the rates of aggregation of unfolded polypeptide chains can be correlated to a remarkable extent with changes in simple physicochemical properties such as hydrophobicity, secondary structure propensity and charge. This approach allows the pathogenic effects of mutations associated with known familial forms of protein deposition diseases to

be rationalized, and more generally enables prediction of the effects of mutations on the aggregation propensity of any polypeptide chain.

The ability to form highly organized aggregates such as the fibrils and plaques associated with the amyloid diseases has been suggested to be a generic property of polypeptide chains, and not simply a feature of the small numbers of proteins so far associated with recognized pathological conditions[5]. Nevertheless, the propensity of a given polypeptide chain to aggregate under specific conditions varies dramatically with its composition and sequence. The proposed generic nature[5] and well established common structural characteristics of aggregates formed from proteins without detectable sequence or structural similarity[6] have encouraged us to investigate whether the effects of amino acid substitutions on the propensity of proteins to aggregate can be described by relatively simple principles that are of general validity. When a protein that is normally folded starts to aggregate, it does so from at least partially unfolded states that are present during or immediately following biosynthesis, or as the result of cellular stress or proteolytic degradation[2,3].

Destabilization of the native state that results in an increased population of partially folded molecules is well established as an important factor in the pathogenic effects of mutations, when the diseases are associated with the deposition of proteins that are globular in their normal functional states[2]. Nevertheless, this factor is not sufficient to explain the pathogenic effects of all mutations associated with such proteins[7,8], in part because the mutations also affect the properties of their aggregation-prone unfolded or partially unfolded states. Clarifying such additional factors that modulate aggregation from non-native states is of fundamental importance for a complete understanding of the relationship between mutation and aggregation behaviour for these systems. More importantly, however, the peptides and proteins
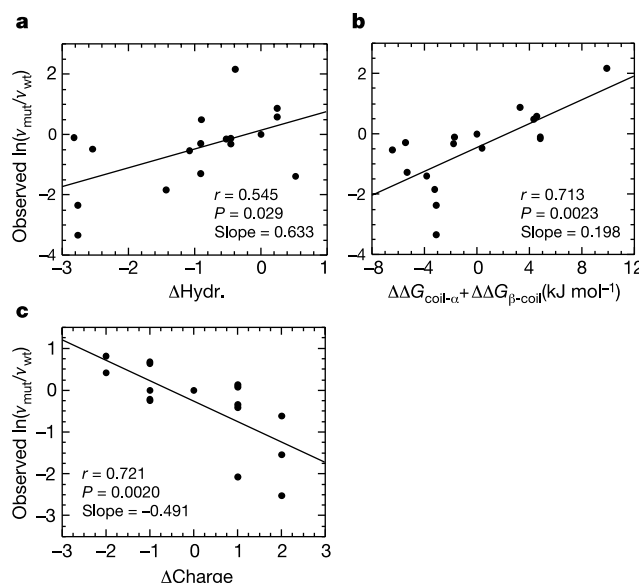
Figure 1 Dependence of the aggregation rate on different physicochemical parameters. Change of the aggregation rate of AcP resulting from mutation plotted against **a**, the predicted change of hydrophobicity, **b**, propensity to convert from an α-helical to a β-sheet conformation, and **c**, charge. All aggregation rate measurements were carried out under conditions in which all the protein variants are substantially unstructured. The mutations reported in **a** and **b**, described previously[9], involve residues 16–31 and 87–98 and do not involve change of charge. The mutations reported in **c**, also described previously[10], were designed to minimize change of hydrophobicity and secondary structure propensities. Values of ΔHydr., ($\Delta\Delta G_{coil-\alpha} + \Delta\Delta G_{\beta-coil}$) and ΔCharge were calculated for each mutation as described in Table 1 legend.